

A dislocation-based constitutive description of strain-rate effect on the deformation resistance of metals

M. C. Cai · H. J. Shi · T. Yu

Received: 19 March 2010 / Accepted: 30 August 2010 / Published online: 9 September 2010
© Springer Science+Business Media, LLC 2010

Abstract A dislocation-based model is presented to study the strain-rate effect on the deformation resistance of metals over a wide range of strain rates. The model is able to take into account the multi-mechanisms, such as dislocation generation, viscous drag, and thermal activation. The results reveal that at high temperatures, the mechanism of viscous drag may play a more significant role than the thermal activation mechanism; whereas at lower temperatures, the viscous drag may be important only under high strain-rate loadings. The cause of deformation instability is also probed. At small plastic strains, deformation instability may be induced by the decrease of the thermally activated stress with increasing deformation. When plastic strains are large, the decreasing of the resistance for dislocation generation with increasing deformation may be the cause.

Introduction

The deformations of metals are usually dominated by the mechanism of thermal activation. The gliding dislocations

can overcome the local barriers with the assistance of thermal fluctuation. In the last 30 years, dislocation theory combined with thermal activation mechanism has been widely used to develop the mechanism-based constitutive relations in literature [1–6]. When the strain rate is larger than a critical value, other deformation mechanisms, such as viscous drag [1–3] and dislocation generation [4, 7], can be important. Armstrong et al. [7] pointed out that for metals deforming under high strain rates with shock loadings, the mechanism of dislocation generation is predominant over viscous drag, and under shockless isentropic loadings, the viscous drag may be distinguished. In order to improve the accuracy of theoretical predictions, in the region of high strain rates, the resistance of viscous drag for dislocation gliding has been introduced into the thermal activation-based constitutive relations. Kocks et al. [8], and subsequently Zerilli and Armstrong [9], considered the resistance of viscous drag coupled with the thermally activated term, whereas Kapoor and Nemat-Nasser [10] treated the contribution of viscous drag as a long-range resistance, and uncoupled with thermally activated term. Zerilli and Armstrong [9] further showed that the mechanism of viscous drag may produce a region of tensile instability at small strains whatever the strain rate is. For materials under large deformations, the variation of dislocation density can be significant. Voyiadjis and Almasri [3] considered this effect on the thermally activated gliding process, and introduced the effect of plastic strain into the dislocation density. However, under high strain-rate loadings, the coupling between viscous drag and dislocation generation was less studied, and few works took into account the deformation resistance during the formation of new dislocations. This resistance can be important for metals under shock loadings, for which rapid dislocation generation will appear at the propagating shock front.

M. C. Cai (✉) · H. J. Shi · T. Yu
AML, School of Aerospace, Tsinghua University,
Room 1511, Yi Fu Building, Beijing 100084, China
e-mail: cmc31@163.com

H. J. Shi
e-mail: shihj@mail.thu.edu.cn

T. Yu
e-mail: yut05@mails.tsinghua.edu.cn

M. C. Cai
Beijing National Center for Electron Microscopy, Department
of Materials Science and Engineering, Tsinghua University,
Beijing 100084, China

The current study aims at investigating the effects of dislocation generation, viscous drag, and thermal activation on the strain-rate-dependent resistance for deformation, and a constitutive description is presented by adopting the dislocation theory. The deformation instability due to these mechanisms is also treated.

Theory

Thermal activation and viscous drag

The mechanism-based constitutive relation is based on the Orowan equation [11], which establishes the relation between the macro-plastic strain ε and the gliding distance of micro-dislocations l as:

$$\varepsilon = \rho b l, \quad (1)$$

where ρ is the density of dislocations, and b is length of Burgers vector. During the dislocation gliding, both the gliding distance l and the dislocation density ρ may evolve with plastic strain, thus it is convenient to use a rate form of Eq. 1 as:

$$\dot{\varepsilon} = \rho b v + \dot{\rho} b \lambda, \quad (2)$$

where v is the average speed of dislocation gliding. λ is the mean free path of dislocations gliding between thermal barriers. The first term on the right side of Eq. 2, $\rho b v$, represents the contributions of dislocations gliding in the macro-strain rate. The second term, $\dot{\rho} b \lambda$, describes the effects of dislocation generation, by considering the changes of crystal volume as a result of the appearance of dislocations. The contributions of the coupling between the two mechanisms to the strain rate can be neglected, however, the variations of the two terms $\rho b v$ and $\dot{\rho} b \lambda$ are coupled. The decomposition as Eq. 2 has been widely accepted in literature, see, e.g., Colvin et al. [12] and Dorgan and Voyiadjis [13]. The parameter λ is usually chosen as a constant λ_0 for the fixed thermal barriers, or as $1/\sqrt{\rho}$, depending on the dislocation density, for the cases that thermal barriers evolve with dislocation density [14]. A mixed form for λ as $\lambda_0 + 1/\sqrt{\rho}$ can also be found in literature [5].

The local barriers arresting the gliding dislocations can be overcome by the thermal activation mechanism. The relation between the frequency of successful jump ν and the absolute temperature T is in the Arrhenius form [6]:

$$\nu = \nu_0 \exp(-G/kT), \quad (3)$$

where k is Boltzmann constant, and ν_0 is the frequency of basic jump. The thermal activation energy G is usually a function of the thermally activated stress, which satisfies $\tau_{th} = \tau - \tau_{ath}$. Here τ is the applied stress, and τ_{ath} is the

athermal stress resulting from the resistance of crystal lattices and long-range interactions, and is independent of the strain rate. The waiting time t_w for a dislocation to overcome the localized obstacle is the inverse of ν , e.g., $1/\nu$.

The thermal activation energy G in Eq. 3 is a function of the applied stress τ . Kocks proposed a well-known formation for G [8, 15]:

$$G = G_0 [1 - (\tau_{th}/\hat{\tau})^p]^q, \quad (4)$$

where $\hat{\tau}$ is the thermally activated stress at 0 K, and G_0 is the reference activation energy, which describes the barrier strength. The parameters p and q are in the ranges of 0–1 and 1–2, respectively, describing the energy profile of thermal barriers.

After jumping successfully, dislocations will glide in the regions free of barriers, until they are arrested by other barriers. The resistance for dislocation gliding in the barrier-free region mainly comes from the mechanism of viscous drag, and the flying velocity is $v_f = b\tau_f/B$ [16], with B the viscous drag coefficient, and $\tau_f = \tau - \tau_{ath}$ the driving force for dislocation gliding. The corresponding flying time $t_f = \lambda/v_f$, and the average speed of dislocation gliding v in Eq. 2 can be written as [8, 9]:

$$v = \lambda/(t_w + t_f) = \frac{\lambda \nu_0 b \tau_f}{b \tau_f \exp[G(\tau_{th})/kT] + \lambda B \nu_0}. \quad (5)$$

The waiting time t_w decreases as thermally activated stress increases, and approaches its minimum value $1/\nu_0$ at $\tau_{th} = \hat{\tau}$, whereas the flying time t_f always decreases as τ_f increases. It should be noted that τ_f and τ_{th} are the driving terms for the movements of dislocations in the region between gliding barriers and in the vicinity of thermal barriers, respectively. The two terms are identical when the thermally activated stresses τ_{th} are below a critical value $\hat{\tau}$. However, when τ_{th} achieves its maximum value $\hat{\tau}$, the activation energy G equals zero, and the waiting time t_w tends to a constant $1/\nu_0$, whereas the flying time t_f continues decreasing with the increase of the driving term τ_f .

Under low strain rates which result in $t_f \ll t_w$, the thermal activation mechanism will dominate, and with the increase of strain rate, t_w may decrease more rapidly than t_f . Then at high strain rates, the condition $t_w \ll t_f$ may appear, and the dominant mechanism may change to viscous drag.

Generally, the viscous drag coefficient B is a function of the gliding speed v , which is a result of the relativistic effects. The speed-dependent character is especially significant when the gliding speed is around the shear wave speed in the solids [17], under which, however, the macro-strain rate can be considered merely determined by the dislocation generation and the contribution of dislocation gliding can be neglected. This study is mainly focused on investigating the coupling effects of different mechanisms

of dislocation gliding, thus the viscous drag coefficient B is chosen to be independent of the gliding speed. In fact, this assumption is widely adopted in literature and can be applicable for materials deformed with the strain rates up to 10^4 s^{-1} , as shown by Ferguson et al. [18].

Dislocation generation

In order to establish the relation between strain rate $\dot{\epsilon}$ and τ_f , an equation that describes the dislocation generation rate $\dot{\rho}$ in Eq. 2 is acquired.

The evolution of dislocation density ρ with plastic deformation has been widely studied in literature [13, 14, 19–27]. Kocks and Mecking [14, 24] proposed a simplified and widely accepted form as:

$$\dot{\rho} = \left(\frac{1}{b\Lambda} - \kappa\rho \right) \dot{\epsilon}, \quad \text{or} \quad \frac{d\rho}{d\epsilon} = \frac{1}{b\Lambda} - \kappa\rho, \quad (6)$$

where $1/(b\Lambda)$ represents the contribution of fixed Frank–Reed sources, with Λ the corresponding segment length. κ is a constant describing the annihilation process. More complicated forms that consider the effects of strain rate and temperature on κ can be found in literature, e.g., Stainier and co-workers [28, 29] and Mecking et al. [30]. Equation 6 describes the contributions of dislocation multiplication ($1/b\Lambda$) and annihilation ($\kappa\rho$) to the generation rate of dislocation during the gliding process.

Since the dislocation generation $\dot{\rho}$ is usually formed during the process of dislocation gliding, it can be found by recalling Eq. 2 that the strain rate $\dot{\epsilon}$ in Eq. 6 has been included in the contribution of dislocation generation, which is not the case and should be modified. It is noticed that $\dot{\rho}$ in Eq. 6 is directly related to the gliding velocity v rather than to the strain rate $\dot{\epsilon}$. Considering this, it is convenient to replace the strain rate $\dot{\epsilon}$ in Eq. 6 with ρbv , which gives:

$$\dot{\rho} = (\rho/\Lambda - \kappa b\rho^2)v, \quad (7)$$

Combining Eqs. 2 and 7 gives:

$$\dot{\epsilon} = (1 + \lambda/\Lambda - \lambda\kappa b\rho)\rho bv, \quad (8)$$

$$\frac{d\rho}{d\epsilon} = \frac{1/\Lambda - \kappa b\rho}{b[1 + \lambda(1/\Lambda - \kappa b\rho)]}. \quad (9)$$

The term $\lambda/\Lambda - \lambda\kappa b\rho$ in Eq. 8 represents the contribution of dislocation generation $\dot{\rho}$ in Orowan equation.

The average speed v for dislocation gliding in Eq. 5 always increases as τ_f increases, and the dislocation density ρ increases monotonously with the increase of plastic strain. Thus, as long as the dislocation density $\rho(\epsilon)$ is below a critical value ρ_c , with $\rho_c = (1 + \lambda/\Lambda)/(2\lambda\kappa b)$, the gliding velocity v in Eq. 8 would decrease as the plastic strain increases when the strain rate is kept unchanged. This

means that the thermally activated stress may decrease when plastic strain increases. If the decrease of the thermally activated stress is more than the increase of the athermal stress τ_{ath} , the deformation instability may be resulted in. Zerilli and Armstrong [9] believed that the viscous drag mechanism may cause the deformation instability for all strain rates. However, when the dislocation generation effect is considered, it is shown from Eq. 8 that the deformation instability may appear only when the initial dislocation density is below ρ_c . This type of deformation instability can be important for dislocation-free metals under plastic deformations, e.g., as the experiment research reported by Kamada and Tanner [31].

The solution of Eq. 9 gives:

$$\ln\left(\frac{1 - \tilde{\rho}_0}{1 - \tilde{\rho}}\right) + \tilde{\lambda}(\tilde{\rho} - \tilde{\rho}_0) = \tilde{\epsilon}, \quad (10)$$

where the dimensionless parameters are $\tilde{\rho} = \rho/\rho_s$, $\tilde{\rho}_0 = \rho_0/\rho_s$, $\tilde{\epsilon} = \kappa\epsilon$, and $\tilde{\lambda} = \lambda/\Lambda$, with ρ_0 the initial dislocation density, $\rho_s = (\Lambda\kappa b)^{-1}$ the saturated dislocation density, and $\rho_c = (1 + \tilde{\lambda}^{-1})(\rho_s/2)$ the critical dislocation density, below which the deformation may be instable. Equation 10 describes the relation between the dislocation density ρ and the plastic strain ϵ , with parameters ρ_s , $\tilde{\lambda}$, and κ .

Substituting Eqs. 4 and 5 into 9, the dimensionless strain rate can be obtained as:

$$\dot{\tilde{\epsilon}} = \tilde{\lambda}\tilde{\rho} \left[1 + \tilde{\lambda}(1 - \tilde{\rho}) \right] \left[\exp(\tilde{g}(1 - \tilde{\rho})^q) + \theta/\tilde{\tau} \right]^{-1}, \quad (11)$$

where $\dot{\tilde{\epsilon}} = \kappa(\dot{\epsilon}/v_0)$ is the derivative of $\tilde{\epsilon}$ with respect to the dimensionless time $\tilde{t} = v_0 t$. The parameters are defined as $\tilde{g} = G_0/kT$, $\tilde{\tau} = \tau_f/\hat{\tau}$, and $\theta = \lambda B v_0 / (b\hat{\tau})$ which is dimensionless. The function $\langle x \rangle$ satisfies $\langle x \rangle = x$ for $x \geq 0$ and $\langle x \rangle = 0$ for $x < 0$. The term $\tilde{\lambda}(1 - \tilde{\rho})$ on the right side of Eq. 11 represents the effects of dislocation generation on strain rate, and is what makes our relation different from those existing ones, e.g., that proposed by Zerilli and Armstrong [9]. Using Eq. 10, the constitutive relation which accounts for the effects of strain rate, temperature and plastic strain can be derived as $\tau = \tau_{ath}(\epsilon, T) + \tau_f(\epsilon, \dot{\epsilon}, T)$.

In order to determine the range of the model parameters in Eq. 11, we will investigate the effects of the model parameters on the transition of the deformation mechanism between thermal activation and viscous drag in the following section.

The transition of deformation mechanism between thermal activation and viscous drag

The parameter $\theta = \lambda B v_0 / (b\hat{\tau})$ in Eq. 11 is important in determining the transition of the deformation mechanism between thermal activation and viscous drag, since the

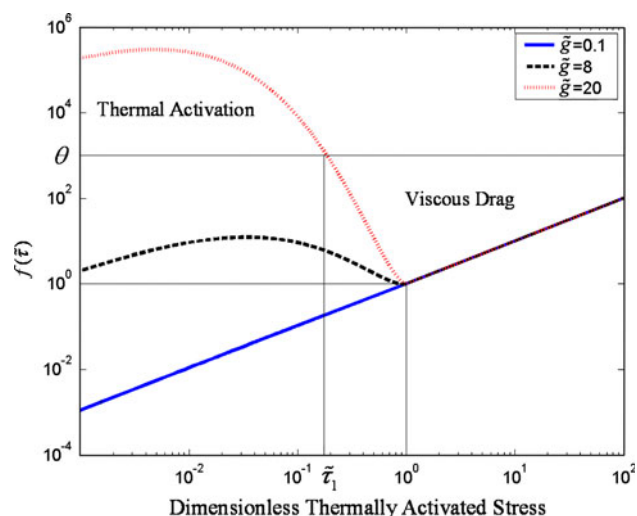


Fig. 1 The evolution of $f(\tilde{\tau})$ with $\tilde{\tau}$ at different values of \tilde{g} , with $p = 0.5$, $q = 1.5$

effects of viscous drag coefficient B , activation frequency ν_0 , and thermal barrier strength $\hat{\tau}$ are reflected. When the term $f(\tilde{\tau}) = \tilde{\tau} \exp(\tilde{g}\langle 1 - \tilde{\tau}^p \rangle) \gg \theta$, the dislocation gliding is governed by the mechanism of thermal activation, and when $f(\tilde{\tau}) \ll \theta$, the mechanism of viscous drag may dominate. The variations of $f(\tilde{\tau})$ with $\tilde{\tau}$ for different values of \tilde{g} are shown in Fig. 1, with $p = 1/2$, $q = 3/2$, and $\tilde{g} = 0.1, 8, 20$, respectively. When $\tilde{\tau} \geq 1$, dislocations can overcome the thermal barriers with frequency, ν_0 and $f(\tilde{\tau})$ is independent of \tilde{g} . When $\tilde{\tau} < 1$, the evolution of $f(\tilde{\tau})$ can be differentiated into two groups according to the value of \tilde{g} . When \tilde{g} is below the critical value \tilde{g}_c , $f(\tilde{\tau})$ increases with the increase of $\tilde{\tau}$ monotonically, whereas if $\tilde{g} > \tilde{g}_c$, with the increase of $\tilde{\tau}$, $f(\tilde{\tau})$ would increase at the beginning and may decrease after some value of $\tilde{\tau}$; when $\tilde{\tau}$ approaches 1, $f(\tilde{\tau})$ will increase again. The critical value \tilde{g}_c can be derived as follows:

$$\tilde{g}_c = \frac{1}{p} (1 - 1/q)^{-q+1}, \tag{12}$$

which only depends on the parameters p and q of the activation energy profile. The contours of \tilde{g}_c are shown in Fig. 2. It can be found that the value of \tilde{g}_c is sensitive to p , which is in accordance with Kocks [15].

For most metallic materials, $\tilde{g} > \tilde{g}_c$, and θ is larger than 1 as well as below the maximum value of $f(\tilde{\tau})$ in the region that $\tilde{\tau} < 1$. This corresponds to the condition of strong thermal barriers and is commonly a viscous medium case. In the region that $\tilde{\tau} < 1$, if $f(\tilde{\tau}) \gg \theta$, the deformations are dominated by the mechanism of thermally activated gliding.

When $\tilde{\tau}$ increases to a value $\tilde{\tau}_1$ and $f(\tilde{\tau}_1) = \theta$ is satisfied, the viscous drag should be considered. This corresponds to the transition of the deformation mechanism between

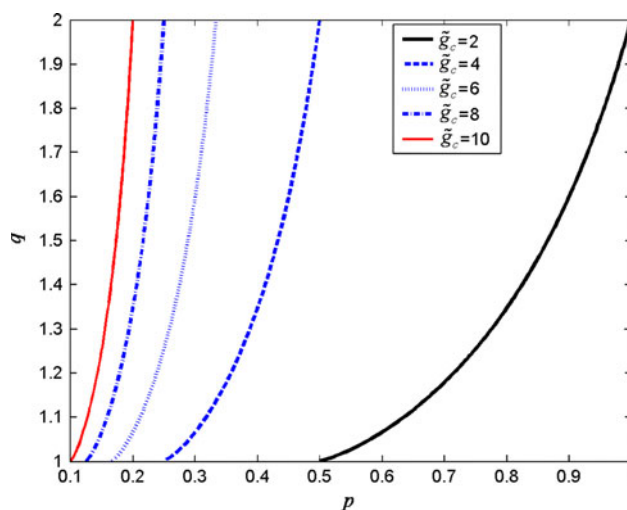


Fig. 2 The relation between the critical value g_c and parameters p and q in Kocks model

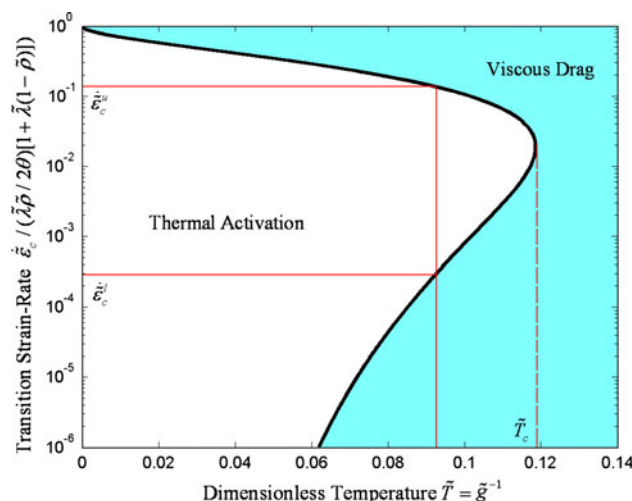


Fig. 3 Variation of the critical strain rate $\dot{\epsilon}_c$ with dimensionless temperature

thermally activated gliding and viscous drag, and the corresponding critical strain rate for transition can be written as $\dot{\epsilon}_c = \tilde{\lambda} \tilde{\rho} (\tilde{\tau}_1 / 2\theta) [1 + \tilde{\lambda} (1 - \tilde{\rho})]$. The strain rate for transition $\dot{\epsilon}_c$ is proportional to $\tilde{\tau}_1$, which implicitly depends on temperature T through \tilde{g} for a given material. Figure 3 shows the variation of $\dot{\epsilon}_c$ (or $\tilde{\tau}_1$) with the dimensionless temperature $\tilde{T} = T(k/G_0) = 1/\tilde{g}$, with parameters $p = 1/2$, $q = 3/2$, and $\theta = 10$. It can be found that with the increase of temperature, the critical strain rate $\dot{\epsilon}_c$ gradually decreases, and when the temperature becomes larger than a critical value \tilde{T}_c , the thermal activation-dominated region may vanish, and the viscous drag may dominate for all strain rates. It should be noted that under high temperature below \tilde{T}_c , there exist two values of $\dot{\epsilon}_c$, denoted as $\dot{\epsilon}_c^l$ and $\dot{\epsilon}_c^u$

($\dot{\epsilon}_c^u > \dot{\epsilon}_c^l$), respectively. The mechanism of viscous drag may play a more important role than thermal activation for materials under both ranges of strain rate: $\dot{\epsilon} < \dot{\epsilon}_c^l$ and $\dot{\epsilon} > \dot{\epsilon}_c^u$. Things are different for the cases under room or low temperatures where only under high strain-rate loadings, the viscous drag is important.

However, if θ is larger than the maximum value of $f(\tilde{\tau})$ in the region of $\tilde{\tau} < 1$, the viscous drag may dominate the dislocation gliding in the entire range of strain rate. This corresponds to the case of an extremely viscous medium. $\theta < 1$ corresponds to the case of a weakly viscous medium, and $f(\tilde{\tau})$ can be larger than θ in most regions of stress. The waiting time t_w is rather long, and the mechanism of thermal activation can be important over a wide range of strain rates. $\tilde{g} < \tilde{g}_c$ corresponds to weak thermal barriers, in which $f(\tilde{\tau})$ increases with the increase of $\tilde{\tau}$ monotonically, and if $\theta > 1$, the viscous drag resistance cannot be neglected.

It should be noted that if $\theta > 1$, $\tilde{\tau}_2 > 1$ holds for $\theta = f(\tilde{\tau})$ that corresponds to the stress up to which the waiting time $t_w = 1/v_0$ is longer than the flying time t_f . In this region, the viscous coefficient B cannot be considered as a constant, and the effects of velocity on B should be considered [16].

Effects of plastic strain

During the loading process, the evolution of dislocation density with plastic deformation may have additional effects on the resistance for deformation. The effects of plastic strain on deformation resistance can be classified into two groups. The first is due to the interaction between gliding dislocations and other dislocations, which may increase along with the dislocation density, and contributes to the resistance for dislocation gliding. This effect is known as strain hardening. Taylor [32] suggested using the following equation to describe the contribution of strain hardening to the deformation resistance as:

$$\tau = \alpha\mu\sqrt{\rho}. \tag{13}$$

Another effect is that the evolution of dislocation density may result in strengthening of the thermal barriers. This effect is coupled with the thermally activated gliding process, and can be taken into account through the evolution equation of the parameter $\hat{\tau}$ by Eq. 4. Voce [33] proposed the following equation:

$$\frac{d\hat{\tau}}{d\varepsilon} = \eta \frac{\hat{\tau}_s - \hat{\tau}}{\hat{\tau}_s - \hat{\tau}_0}, \tag{14}$$

where $\hat{\tau}_0$ and $\hat{\tau}_s$ are the initial and saturated values of $\hat{\tau}(\varepsilon)$, respectively. The hardening rate of $\hat{\tau}$ in Voce model decreases linearly with the increase of $\hat{\tau}$. Other nonlinear

forms of the evolution equation can be found in literature, e.g., Preston et al. [34] and Gourdin and Lassila [35].

Integrating Eq. 14 with respect to the plastic strain ε gives:

$$\hat{\tau} = \hat{\tau}_s - (\hat{\tau}_s - \hat{\tau}_0) \exp[-\varepsilon\eta/(\hat{\tau}_s - \hat{\tau}_0)]. \tag{15}$$

By considering these effects, the deformation resistance can be written as:

$$\tau = \tau_0 + \alpha\mu\sqrt{\rho} + \tau_{th}(\dot{\epsilon}, T, \hat{\tau}), \tag{16}$$

where τ_0 is a constant. The thermally activated stress $\tau_{th}(\dot{\epsilon}, T, \hat{\tau})$ in Eq. 16 can be obtained using Eq. 11, and the effects of plastic strain on thermally activated stress τ_{th} is implicitly introduced through $\hat{\tau}$ in Eq. 15.

Resistance of dislocation generation for deformation

In the previous sections, the deformation resistances of dislocation gliding (thermal activation and viscous drag) and plastic strain effects are investigated. During the dislocation gliding, the formation of geometrically necessary dislocations may give an additional resistance for deformation: τ_ρ .

Armstrong and Zerilli [7] suggested to use a thermal-activation-type equation to describe $\dot{\rho}$, which is similar to Eq. 3, and the difference between the deformation resistance of dislocation generation and the thermally activated gliding can be attributed to the difference in activation volume, which is defined as $V \equiv -\partial G/\partial\tau_{th}$.

During the dislocation generation process with rate $\dot{\rho}$, the power needed to produce dislocations in a unit volume $\dot{\rho}U_\rho$ is supplied by τ_ρ , where U_ρ is the energy needed to form a unite length of dislocation. By neglecting the contributions of kinetic energy, and considering the energy conservation, we obtain:

$$\dot{\rho}U_\rho = \tau_\rho v, \tag{17}$$

where v is the average speed for dislocation gliding in Eq. 2. Substituting Eq. 7 into 17 gives:

$$\tau_\rho = (\rho/\Lambda - \kappa b\rho^2)U_\rho. \tag{18}$$

By counting the contribution of τ_ρ into Eq. 16, the total resistance for deformation can be written as:

$$\tau = \tau_0 + \alpha\mu\sqrt{\rho} + (\rho/\Lambda)(1 - \rho/\rho_s)U_\rho + \tau_{th}(\dot{\epsilon}, T, \hat{\tau}). \tag{19}$$

The athermal component stress in Eq. 19 corresponds to:

$$\tau_{ath} = \tau_0 + \alpha\mu\sqrt{\rho} + (\rho/\Lambda)(1 - \rho/\rho_s)U_\rho, \tag{20}$$

which may evolve with the plastic strain through the dislocation density ρ .

Under shock loadings, the parameter Λ in Eq. 7 may be smaller than that under shockless isentropic loadings. Thus

at the same deformation stage (with the same macro-plastic strain), shock loadings may result in a dramatically larger dislocation density than shockless isentropic loadings. Consequently, the athermal stress in Eq. 20 corresponding to a deformation dominated by dislocation generation should be larger than that by viscous drag. For a shockless isentropic loading, the opposite is true.

Discussion

Effects of strain rate on flow stress

The mechanism of viscous drag is widely adopted to explain the upturns in the curves of strain rate and flow stress at regions of high strain rate [7]. Zerilli and Armstrong [9] introduced the mechanism of viscous drag into a thermal activation-based model (Z–A model), to capture the strain-rate dependent flow stress at regions of high strain rates. Figure 4 shows the comparison between the predictions by the present model and the Zerilli and Armstrong model [9], with the experimental results of copper from [2] at the strain $\varepsilon = 0.15$. The model parameters in Eq. 11 are chosen as $p = 2/3$, $q = 2$, $\tilde{g} = 68$, which are the same as those used by Nemat-Nasser and Li [36]. The other parameters are $\theta = 8$, $\hat{\tau} = 200$ MPa, $\tau_{\text{ath}} = 140$ MPa, and $\tilde{\lambda}\tilde{\rho}(v_0/\kappa)[1 + \tilde{\lambda}(1 - \tilde{\rho})] = 2 \times 10^5$. It can be found that the prediction by the present model is closer to the experimental result than by Zerilli and Armstrong model.

In “Dislocation generation,” we have discussed that with the increase of plastic strain, the thermally activated stress

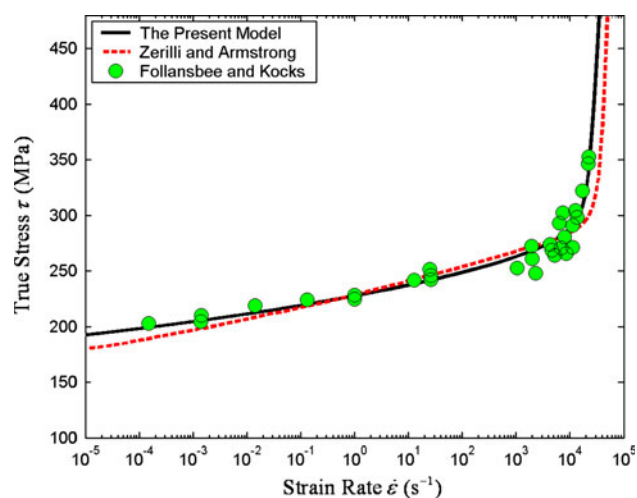


Fig. 4 Comparison between the predictions by the present model and the Zerilli and Armstrong model [9] with the experimental results by Follansbee and Kocks [2], under $\varepsilon = 0.15$

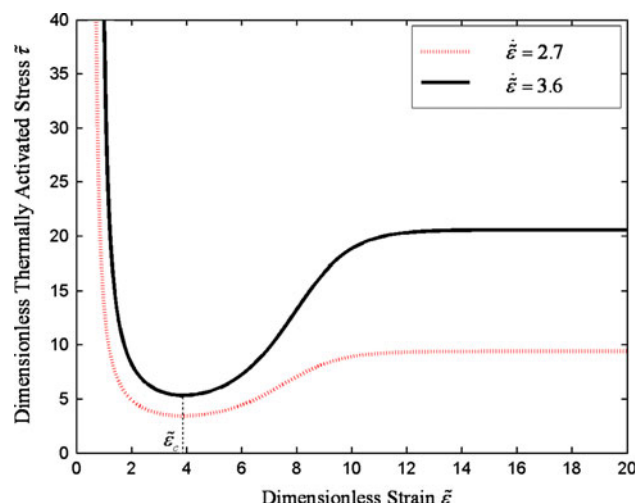


Fig. 5 Variation of dimensionless thermally activated stress $\tilde{\tau}$ with dimensionless plastic strain $\tilde{\varepsilon}$

should decrease for dislocation density below a critical value ρ_c (corresponding to the dimensionless value $\tilde{\rho}_c = \rho_c/\rho_s = (1 + \tilde{\lambda}^{-1})/2$). The evolution of dislocation density with plastic strain is governed by Eq. 10. For simplification, we choose the initial dislocation density $\tilde{\rho}_0 = 0$ in Eq. 10, and $\eta = 0$ in Eq. 14 in the following discussion. Under these assumptions, $\hat{\tau}$ can be considered a constant, and $\tilde{\rho}$ is always below the critical value $\tilde{\rho}_c$ at the initial of plastic deformations. Based on Eq. 10, the plastic strain corresponding to $\tilde{\rho}_c$ can be obtained as $\tilde{\varepsilon}_c = \tilde{\lambda}\tilde{\rho}_c - \ln(1 - \tilde{\rho}_c)$. Figure 5 shows the variation of the dimensionless thermally activated stress $\tilde{\tau}$ with dimensionless strain $\tilde{\varepsilon}$, based on Eqs. 10 and 11, with the dimensionless strain rate $\tilde{\varepsilon} = 2.7$ and 3.6 , respectively. In Fig. 5, the parameters p , q , θ , and \tilde{g} are the same as those used in Fig. 4, and $\tilde{\rho}_c = 0.6$ (corresponding to $\tilde{\lambda} = 5.0$). At the beginning of plastic deformation, since $\tilde{\rho} = 0$, the materials are free of dislocations, and the deformation resistance is close to its theoretical strength. When the initial dislocation density $\tilde{\rho}_0$ is above zero, and is below the critical value $\tilde{\rho}_c$, the dimensionless thermally activated stress $\tilde{\tau}$ dramatically decreases with the increase of plastic strain $\tilde{\varepsilon}$, and may result in deformation instability. If $\tilde{\rho}_0 \geq \tilde{\rho}_c$, $\tilde{\tau}$ always increases with an increasing plastic strain, and the metals may deform stably. The dimensionless thermally activated stress $\tilde{\tau}$ in Fig. 5 depends on the plastic strain, until the dislocation density reaches its saturated value ρ_s (i.e., $\tilde{\rho} = 1$). The increase of the thermally activated stress due to the increase of the strain rate depends on the plastic strain, which means that the value $m = \partial\tilde{\tau}/\partial\tilde{\varepsilon}$ can increase along with the plastic strain, and can gradually tend to a constant when $\tilde{\rho}$ approaches 1.

Effects of dislocation generation on the long-range resistance

With the increase of plastic deformation, the evolution of dislocation density may lead to two additional long-range deformation resistances, i.e., the resistance for the interactions between dislocations, $\tau_i = \alpha\mu\sqrt{\rho}$, and for the generation of new dislocations, $\tau_\rho = (\rho/A)(1 - \rho/\rho_s)U_\rho$, as discussed in “Effects of plastic strain” and “Resistance of dislocation generation for deformation.” The latter can be important for materials under shock loadings, with a small value of A corresponding to fast dislocation generation. The corresponding resistance for deformation may decrease with the increase of deformation, if the dislocation density ρ becomes larger than $\rho_s/2$, i.e., $\tilde{\rho} > 1/2$. That may result in the deformation instability.

Using Eq. 20, the dimensionless form for the athermal stress can be written as:

$$\tilde{\tau}_{ath} = \tilde{\tau}_0 + \tilde{\tau}_i + \tilde{\tau}_\rho = \tilde{\tau}_0 + \zeta\sqrt{\tilde{\rho}} + \xi\tilde{\rho}(1 - \tilde{\rho}), \quad (21)$$

where $\tilde{\tau}_{ath} = \tau_{ath}/\hat{\tau}$, $\tilde{\tau}_0 = \tau_0/\hat{\tau}$, $\tilde{\tau}_i = \tau_i/\hat{\tau} = \zeta\sqrt{\tilde{\rho}}$, $\tilde{\tau}_\rho = \tau_\rho/\hat{\tau} = \xi\tilde{\rho}(1 - \tilde{\rho})$, and the parameters $\zeta = \alpha(\mu/\hat{\tau})\sqrt{\rho_s}$, and $\xi = (\rho_s U_\rho/\hat{\tau}A)$. Figure 6 shows the variation of dimensionless athermal stress $\tilde{\tau}_{ath}$ with dimensionless plastic strain $\tilde{\epsilon}$, with parameters set as $\zeta = 10$, $\xi = 40$, and $\tilde{\rho}_c = 0.6$.

Both the variations of thermally activated stress τ_{th} and the resistance for dislocation generation τ_ρ with the increase of plastic strain may lead to deformation instability. However, Eq. 11 reveals that the former condition may appear for the dimensionless dislocation density $\tilde{\rho}$ below $\tilde{\rho}_c$, and larger than $1/2$, whereas the latter may appear for $\tilde{\rho} > 1/2$. Thus, the deformation instability may be in response to the decrease of thermally activated stress

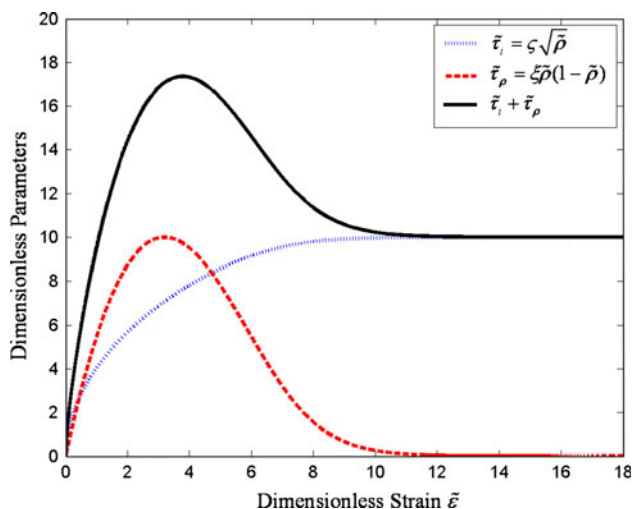


Fig. 6 Variation of $\tilde{\tau}_i$, $\tilde{\tau}_\rho$ and $\tilde{\tau}_{ath} - \tilde{\tau}_0 = \tilde{\tau}_i + \tilde{\tau}_\rho$ with dimensionless plastic strain $\tilde{\epsilon}$

$\tilde{\tau}$, for small plastic strain ($\tilde{\rho} < 1/2$), and to the decrease of $\tilde{\tau}_\rho$, for larger deformation ($\tilde{\rho} > \tilde{\rho}_c$). These two causes can coexist for materials deforming under high strains, e.g., the experimental results of annealed tantalum reported by Hoge and Gillis [37].

Conclusion

A dislocation-based model is presented to study the strain-rate-dependent behavior of materials, with multi-mechanisms counted in, such as dislocation generation, viscous drag, and thermal activation. The results show that the strain rate corresponding to the transition of deformation mechanism between viscous drag and thermal activation decreases with increasing temperature. Besides, the viscous drag mechanism may play a more important role than the thermal activation for materials deforming under high temperature and both regions of low and high strain rates. There are two mechanisms for deformation instability: the decrease of thermally activated stress is dominant for small deformations (with low dislocation density), and the decrease of the resistance for deformation contributed by dislocation generation answers for the deformation instability occurred under large deformations. The athermal stress for deformation dominated by dislocation generation is larger than that by viscous drag for materials under high strain-rate loadings, and the condition for thermally activated stress is the opposite.

Acknowledgements The authors thank the financial support from the Joint Foundation of the National Natural Science Foundation of China and China Academy of Engineering Physics (NSAF Project) under Grant No. 10776019, the National Basic Research Program of China through Grant No. 2010CB631005, and the Open Foundation of State Key Laboratory of Explosion Science and Technology (Beijing Institute of Technology, China, Grant No. KFJ08-9).

References

1. Zerilli FJ, Armstrong RW (1987) J Appl Phys 61:1816
2. Follansbee PS, Kocks UF (1988) Acta Metall Mater 36:81
3. Voyiadjis GZ, Almasri AH (2008) Mech Mater 40:549
4. Armstrong RW, Arnold W, Zerilli FJ (2007) Metall Mater Trans A 38:2605
5. Zerilli F (2004) Metall Mater Trans A 35:2547
6. Kocks UF, Mecking H (2003) Prog Mater Sci 48:171
7. Armstrong RW, Arnold W, Zerilli FJ (2009) J Appl Phys 105:023511
8. Kocks UF, Argon AS, Ashby MF (1975) Thermodynamics and kinetics of slip. Pergamon, Oxford
9. Zerilli FJ, Armstrong RW (1992) Acta Metall Mater 40:1803
10. Kapoor R, Nemat-Nasser S (2000) Metall Mater Trans A 31:815
11. Orowan E (1940) Proc Phys Soc 52:8
12. Colvin JD, Minich RW, Kalantar DH (2009) Int J Plast 25:603
13. Dorgan RJ, Voyiadjis GZ (2003) Mech Mater 35:721
14. Arsenlis A, Wirth BD, Rhee M (2004) Philos Mag 84:3617

15. Kocks UF (2001) *Mater Sci Eng A* 317:181
16. Gilman JJ (2000) *Metall Mater Trans A* 31A:811
17. Gillis PP, Gilman JJ, Taylor JW (1969) *Philos Mag* 20:279
18. Ferguson WG, Hauser FE, Dorn JE (1967) *Br J Appl Phys* 18:411
19. Ananthakrishna G (2007) *Phys Rep* 440:113
20. Fressengeas C, Beaudoin AJ, Lebyodkin M, Kubin LP, Estrin Y (2005) *Mater Sci Eng A* 400–401:226
21. Zikry MA, Kao M (1996) *J Mech Phys Solids* 44:1765
22. Jawad FF, Zikry MA (2009) *Int J Damage Mech* 18:341
23. Ma J, Zikry M (2009) *Rev Adv Mater Sci* 19:78
24. Kocks UF (1976) *ASME J Eng Mater Tech* 98:76
25. Bammann DJ, Mosher D, Hughes DA, Moody NR, Dawson PR (1999) Sandia National Laboratories Report, SAND99-8588
26. Hochrainer T, Zaiser M, Gumbsch P (2007) *Philos Mag* 87:1261
27. Zaiser M, Nikitas N, Hochrainer T, Aifantis EC (2007) *Philos Mag* 87:1283
28. Stainier L, Cuitino AM, Ortiz M (2003) *J Phys IV* 105:157
29. Cuitino AM, Stainier L, Wang G, Strachan A, Cagin T, Goddard WA, Ortiz M (2001) *J Comput Aided Mater Des* 8:127
30. Mecking H, Nicklas B, Zarubova N, Kocks UF (1986) *Acta Metall Mater* 34:527
31. Kamada K, Tanner BK (1974) *Philos Mag* 29:309
32. Taylor GI (1934) *Proc R Soc Lond A* 145:362
33. Voce E (1948) *J Inst Met* 74:537
34. Preston DL, Tonks DL, Wallace DC (2003) *J Appl Phys* 93:211
35. Gourdin WH, Lassila DH (1996) TMS Annual meeting and exhibition of the Minerals, Anaheim
36. Nemat-Nasser S, Li Y (1998) *Acta Mater* 46:565
37. Hoge K, Gillis P (1971) *Metall Mater Trans B* 2:261